FEBS Letters 584 (2010) 4339–4343

journal homepage: www.FEBSLetters.org

Ammonia permeability of the soybean nodulin 26 channel

Jin Ha Hwang [a], Sally R. Ellingson [a], Daniel M. Roberts [a,b,*]

[a] Graduate School of Genome Science and Technology, The University of Tennessee-Oak Ridge National Laboratory, Oak Ridge, TN 37830, USA
[b] Department of Biochemistry and Cellular and Molecular Biology, The University of Tennessee, Knoxville, TN 37996, USA

ARTICLE INFO

Article history:
Received 8 August 2010
Revised 10 September 2010
Accepted 22 September 2010
Available online 26 September 2010

Edited by Julian Schroeder

Keywords:
Nitrogen fixation
Aquaporin
Symbiosis
Legume

ABSTRACT

Soybean nodulin 26 (nod26), a member of the aquaporin superfamily, is the major protein component of the symbiosome membrane that encloses nitrogen-fixing bacteroids in root nodules. Previous work has demonstrated that nod26 facilitates the transport of water and glycerol, although a potential additional role as a channel for fixed ammonia efflux has been hypothesized. In the present study it is shown that recombinant nod26 reconstituted into proteoliposomes facilitates NH_3 transport in an Hg^{2+}-sensitive manner with a reduced activation energy, hallmarks of protein-facilitated transport characteristic of aquaporins. Comparison of the predicted single-channel transport rates of nod26 suggests a 4.9-fold preference for ammonia compared to water.

1. Introduction

During the infection and nodulation of legume roots by soil bacteria of the Rhizobiaceae family, the invading endosymbiont becomes enclosed within a specialized nitrogen-fixing organelle known as the "symbiosome" [1]. In mature nodules the host infected cells are occupied by thousands of symbiosomes, which constitute the major organelle within this specialized cell type. The symbiosome membrane (SM), also referred to as the peribacteroid membrane, is the outer boundary of this organelle which controls the transport of metabolites between the symbiont and the plant host [2]. These transport activities include the efflux of the primary metabolic product of nitrogen fixation (NH_3/NH_4^+) and the uptake of dicarboxylates as an energy source to support bacterial N_2 fixation [2,3].

Because of the specialized function of the SM, a number of host nodulin proteins are synthesized and localized to this membrane, and serve transport and regulatory functions in the symbiosis [4,5]. Soybean nodulin 26 (nod26) is among this collection of SM nodulins [6]. Nod26 is a member of the major intrinsic protein (MIP)/aquaporin superfamily of integral membrane protein channels, and it constitutes the major protein component, accounting for >10% of the total SM protein mass [7,8]. Functional analyses show that nod26 is a multifunctional "aquaglyceroporin" that transports multiple substrates including water, formamide, and glycerol [8,9]. As a SM-specific aquaglyceroporin, nod26 has been suggested to serve as a low-energy transport pathway for water as well as osmolytes within the infected cell, potentially to aid in cell volume regulation, and to facilitate infected cell adaptation to osmotic stresses [10]. However, given its multifunctional transport activity, a role in infected cell metabolism cannot be excluded. In particular, work by Niemietz and Tyerman [11] with isolated SM vesicles provided support for a facilitated pathway of NH_3 transport that is inhibited by Hg^{2+}. Since the aquaporin activity of nod26 is also blocked by Hg^{2+} [8,9] and considering that a number of aquaporins show permeability to ammonia [12–14], a potential additional transport activity for nod26 may be the transport of fixed nitrogen in the form of NH_3 from the symbiosome [11]. In the present paper we have tested this hypothesis by investigating the quantitative NH_3 transport properties of purified nod26 reconstituted into proteoliposomes.

2. Materials and methods

2.1. Molecular cloning techniques

The nod26 ORF was obtained from nodule cDNA by PCR amplification with the following primer set:

Forward, CAGGATCCACCATG**CATCACCACCACCATCAT**ATGGCTG
ATTATTCAGCAGG

Abbreviations: CF, carboxyfluorescein; MIP, major intrinsic protein; Nod26, soybean nodulin 26; OG, *n*-octyl-β-D-glucopyranoside; SM, symbiosome membrane; TEM, transmission electron microscopy

* Corresponding author at: Department of Biochemistry and Cellular and Molecular Biology, The University of Tennessee, Knoxville, TN 37996, USA. Fax: +1 865 974 6306.
E-mail address: drobert2@utk.edu (D.M. Roberts).

0014-5793/$36.00
doi:10.1016/j.febslet.2010.09.033

Reverse, GTATTCAATGCGGCCGCCTATTATTTGGAGGCAGCACGG CCTTTGA

The BamHI and NotI restriction sites are underlined and the region encoding a six histidine amino terminal tag is shown in bold. The PCR product was cloned into BamHI and NotI digested pPIC3.5 K (Invitrogen) which was transformed into *Escherichia coli* DH5α and positive clones were verified by DNA sequencing of purified plasmid samples by using a Perkin–Elmer Applied Biosystems 373 DNA sequencer at the University of Tennessee Molecular Biology Research Facility (Knoxville, TN). For *Pichia pastoris* transformation, plasmid samples were linearized by digestion with SacI and transformed into *P. pastoris* GS115 by electroporation as described in [15].

2.2. Recombinant nod26 purification and reconstitution

Transformants expressing nod26 were selected by growth on histidine-deficient minimal dextrose agar plates and the clones with the highest nod26 expression were identified by immunoblotting with nod26 antibodies [10]. *P. pastoris* expression clones were cultured and protein expression was induced as described in [16]. Cell pellets obtained from a 1 l culture were resuspended in 40 ml of 20 mM Tris–HCl, pH 8.0, 100 mM NaCl, 0.5 mM EDTA, 5% (v/v) glycerol, 1 μg/ml leupeptin, 1 μg/ml pepstatin A, 0.5 mM phenylmethylsulfonyl fluoride and were lysed in a French-Press Cell Disrupter (Thermo Scientific). The lysate was centrifuged at 7000×*g* for 45 min at 4 °C, and the resultant supernatant fraction was then centrifuged at 200 000×*g* for 1 h at 4 °C. The final pellet fraction was suspended in 40 ml of 5 mM Tris–HCl, pH 9.5, 5 mM EDTA, 5 mM EGTA, 4 M urea with a Dounce homogenizer, and was recentrifuged at 200 000×*g* for 1 h at 4 °C. The membrane pellet was washed with 10 mM Tris–HCl, pH 8.0 and was resuspended in 20 ml of 20 mM Tris–HCl, pH 8.0, 100 mM NaCl, 5% (v/v) glycerol, 20 mM imidazole, 3% (w/v) *n*-octyl-β-D-glucopyranoside (OG), and solubilization of the membrane pellet was done by gentle agitation for 24 h at 4 °C. The mixture was centrifuged at 12 000×*g* for 20 min, and the supernatant fraction was combined with Ni^{2+}-NTA resin (1 ml packed volume) (Qiagen) and was incubated overnight at 4 °C. The resin was washed with 40 volumes of 20 mM Tris–HCl, pH 8.0, 300 mM NaCl, 35 mM imidazole, 1% (w/v) OG. Histidine-tagged nod26 was eluted with 20 mM Tris–HCl, pH 8.0, 300 mM NaCl, 500 mM imidazole, 1% (w/v) OG and was concentrated to 0.5–1.0 mg/ml using a Vivaspin sample concentrator with a 50 kDa MW cutoff (GE healthcare). The concentrated sample was dialyzed for 24 h at 4 °C against of 20 mM Tris–HCl, pH 7.8, 0.9% (w/v) OG, 0.1 mM 2-mercaptoethanol and 1 μM leupeptin and was stored at −80 °C until reconstitution.

Proteoliposome reconstitution was performed by a rapid dilution protocol as previously described [9]. Nod26 (200–250 μg) was combined with 10 mg of bath-sonicated *E. coli* total lipid (Avanti Polar Lipids) in 50 mM Tris–HCl (pH 7.5), 0.125% (w/v) OG in a final volume of 1.0 ml. The mixture was incubated on ice for 30 min, and liposomes were reformed by rapidly injecting the sample into 20 ml of 250 mM sorbitol, 30 mM KCl, 10 mM HEPES-KOH, pH 6.8, 100 μM carboxyfluorescein (CF) at room temperature. The liposome mixture was incubated for 30 min and the liposomes were pelleted by ultracentrifugation at 100 000×*g* for 1.5 h at 4 °C. The liposome pellet was washed with 5 ml of 250 mM sorbitol, 30 mM KCl, 10 mM HEPES-KOH, pH 6.8 and was recentrifuged and resuspended in the same buffer. Negative control liposomes were prepared in a similar manner except nod26 was omitted. The diameters of nod 26 proteoliposomes and liposomes were determined by transmission electron microscopy (TEM) by uranyl acetate negative staining as described in [9]. Vesicle diameters were measured using the ImageJ software (National Institutes of Health).

2.3. Permeability measurements

Permeability measurements for NH_3 uptake in liposomes were performed as described in [11], using an Applied Photophysics model SX stopped-flow spectrofluorimeter (excitation at 492 nm, emission filtered with 515 cut-off filter). Liposome samples (20 μl) in 250 mM sorbitol, 30 mM KCl, 10 mM HEPES-KOH, pH 6.8 were injected into an equivalent volume of 250 mM sorbitol, 30 mM KCl, 10 mM NH_4Cl, 10 mM HEPES-KOH, pH 6.8 and the increase in CF fluorescence resulting from NH_3 uptake and alkalinization of the internal liposome space was monitored. Under the conditions of this experiment, changes of in internal pH were linearly correlated with changes of the relative fluorescence. Data from five injections/sample were averaged. Data obtained in the presence or absence of 4.5 μM valinomycin were identical suggesting that any possible change in membrane potential due to liposome alkalinization does not affect the NH_3 transport rate. To determine P_{NH_3}, the differential equations described by Boron and De Weer [17] were modified based on the parameters of the experimental system used in this study.

$$\frac{d[\mathrm{Am_{total}}]_i}{dt} = \mathrm{SAV}\left[P_{\mathrm{NH_3}}\left([\mathrm{NH_3}]_o - \frac{K_a}{[\mathrm{H^+}]_i + K_a}\cdot[\mathrm{Am_{total}}]_i\right)\right]$$

$$\frac{d[\mathrm{H^+}]_i}{dt} = \frac{-2.303\cdot[\mathrm{H^+}]_i\cdot\mathrm{SAV}}{\beta}\left[-\frac{[\mathrm{H^+}]_i}{[\mathrm{H^+}]_i + K_a}\cdot P_{\mathrm{NH_3}} \times\left([\mathrm{NH_3}]_o - \frac{K_a}{[\mathrm{H^+}]_i + K_a}\cdot[\mathrm{Am_{total}}]_i\right)\right]$$

$[\mathrm{Am_{total}}]_i$ = total concentration of $NH_3 + NH_4^+$ inside the liposome space; $[H^+]_i$ = total proton concentration inside the liposome space; K_a is the equilibrium constant defining NH_4^+ deprotonation ($pK_a = 9.24$); SAV is the surface area to volume ratio of the liposomes; $[NH_3]_o$ is the external concentration of ammonia; β is the buffer capacity of the liposome space; and P_{NH_3} is the ammonia permeability constant. The buffer capacity was measured by monitoring the change in fluorescence (an internal reporter of pH) in response to proton flux via addition of a membrane permeant acid (acetic acid). The system of differential equations was solved numerically in Mathematica 7 (Wolfram) using the experimental conditions to generate set of theoretical curves describing the change in intracellular pH as a function of varying P_{NH_3}. Experimental stopped flow data were fit to a single exponential and were then compared to the theoretical curves to determine permeability values. The single channel rate, p_{NH_3}, for NH_3 flux per nod26 monomer was quantitated by standardizing P_{NH_3} to the surface density of nod26. The amount of nod26 reconstituted into liposomes was quantitated by Western blot with nod26-specific antisera [18] as described in [9]. The osmotic water permeability of liposome preparations was determined by the light scattering technique described in [11].

3. Results

3.1. Purification and reconstitution of nod26 into liposomes

The nod26 ORF was cloned into a *P. pastoris* expression vector translationally fused to an amino terminal His_6-tag driven by the methanol-inducible *AOX1* promoter. Expression clones showing high histidine-tagged nod26 expression were chosen for large scale purification of the protein. Nod26 was solubilized from a microsomal membrane fraction by solubilization in OG and was fractionated by chromatography on Ni-NTA agarose. This yielded a highly

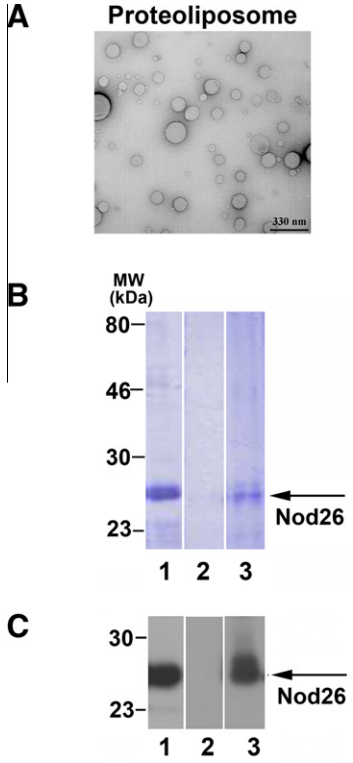

Fig. 1. Purification and reconstitution of recombinant nod26 into proteoliposomes. (A) TEM images of negatively stained nod26-proteoliposomes. Scale bars represent 330 nm. (B) Coomassie blue-stained gel and (C) anti-nod26 Western blot of purified nod26 before reconstitution and liposome preparations after resolution by SDS–PAGE on a 12% (w/v) polyacrylamide gel. Lane 1; purified recombinant nod26 (3 μg) expressed in *P. pastoris*; 2; negative control liposomes, and 3; nod26 proteoliposomes. Arrow indicates predicted molecular weight of histidine-tagged nod26.

purified protein band with an apparent molecular weight of 27 kDa which was identified as nod26 based on Western blot analysis with anti-nod26 antibodies (Fig. 1).

A preparation of single unilammelar vesicle liposomes consisting of purified *E. coli* lipids was generated by bath sonication (Fig. 1). Purified nod26 in OG micelles was combined with this liposome sample and was reconstituted by rapid dilution of the mixture in a buffer containing 100 μM CF to enable loading of the liposome preparations with this pH sensitive dye. Proteoliposomes were collected and washed and the incorporation of nod26 was quantitated by Western blot analysis. The average size of the final liposome preparations was determined by visualization by TEM (Fig. 1, Table 1).

3.2. Ammonia permeability properties of reconstituted nod26 proteoliposomes

The ammonia permeability properties of the CF-loaded proteoliposomes were measured by using stopped-flow fluorimetry upon injection into NH_4^+ containing buffers. Uptake of NH_3 is followed by protonation which results in alkalinization of the liposome space which is accompanied by an increase in CF fluorescence (Fig. 2). From this rate of alkalinization, and taking into account the experimental parameters discussed in the Section 2, nod26 proteoliposomes showed a $P_{NH_3} = 35.1 \pm 2.84 \times 10^{-3}$ cm/s, a rate that is 2.5-fold greater than that exhibited by negative control liposomes ($P_{NH_3} = 13.8 \pm 0.24 \times 10^{-3}$ cm/s) (Fig. 2).

To verify that transport of NH_3 in nod26 proteoliposomes occurs through a protein-based pathway, the effect of Hg^{2+} on transport was assessed (Fig. 2). Previous work has shown that water and solute transport through nod26 is inhibited by Hg^{2+}, presumably by

Table 1
Summary of NH_3 and water permeability properties of liposome preparations.

	Nod26 proteoliposomes	Control liposomes
Diameter (nm)[a]	116 (7.3, $n = 3$)[b]	113 (3.6, $n = 3$)
P_{NH_3} (cm/s) $\times 10^{-3}$[c]	35.1 (2.84, $n = 13$)	13.8 (0.24, $n = 9$)
P_{NH_3} with $HgCl_2$ (cm/s) $\times 10^{-3}$	15.3 (1.81, $n = 8$)	13.2 (1.26, $n = 4$)
Hg^{2+}-sensitive[d] P_{NH_3} (cm/s) $\times 10^{-3}$	19.8	
E_a (kJ/mol)	38.3	90.4
Nod26 surface density (subunits/cm^2) $\times 10^{11}$	8.77 (0.39, $n = 3$)	
p_{NH_3} (cm^3/subunit/s) $\times 10^{-14}$	1.27 (0.06, $n = 3$)	
NH_3 transported per subunit[e] (s^{-1}) $\times 10^9$	0.306	
P_f (cm/s) $\times 10^{-3}$	9.45 (0.65, $n = 19$)	5.54 (0.32, $n = 7$)
P_f with $HgCl_2$ (cm/s) $\times 10^{-3}$	5.15 (0.32, $n = 6$)	
Hg^{2+}-sensitive[d] P_f (cm/s) $\times 10^{-3}$	4.30 $\times 10^{-3}$	

[a] Between 130 and 220 vesicles were measured and averaged for each liposome preparation tested.
[b] The standard error of the means for the indicated number of measurements is shown parenthetically.
[c] The buffer capacity β for both liposome preparations was 15.9 mM/pH unit.
[d] The Hg^{2+} sensitive activity was obtained by subtracting the permeability values obtained in the presence of 1 mM $HgCl_2$ from the uninhibited permeability values.
[e] A molar volume of 24.96 cm^3/mol for NH_3 was used for this calculation.

modification of a critical Cys sulfhydryl [8,9]. Preincubation of nod26 proteoliposomes with 1 mM $HgCl_2$ reduced NH_3 uptake to the level observed with negative control liposomes (Fig. 2). Negative control liposomes were not affected by $HgCl_2$. Another hallmark of MIP-facilitated transport of water and solutes is a reduced Arrhenius activation energy compared to diffusion through a lipid bilayer. Consistent with this prediction, analysis of the NH_3 permeability of nod26 proteoliposomes as a function of temperature shows a low E_a (38.3 kJ/mol) compared with that of control liposomes (90.4 kJ/mol) (Fig. 2).

3.3. Single channel conductance determination and comparison of ammonia and water permeability

To compare the relative selectivity of water and ammonia transport of nod26, the osmotic water permeability (P_f) was evaluated by stopped flow spectroscopy upon injection into hyperosmotic buffers by using light scattering as an index of liposome shrinkage as described previously [11]. This allows direct comparison of the P_{NH_3} and P_f constants for the same liposome preparations. Consistent with previous reports, reconstitution of nod26 into proteoliposomes results in enhanced water permeability which exhibits Hg^{2+} sensitivity (Fig. 3).

To standardize and compare the ammonia and water transport rates, single channel transport permeabilities were calculated based on the surface density of nod26 on proteoliposomes. Since the permeability constant is a combination of protein based transport (Hg^{2+}-sensitive) and lipid bilayer diffusion (Hg^{2+}-insensitive), the calculation of the single channel rate was based on the Hg^{2+}-sensitive fraction of ammonia or water transport (Table 1). By this approach, a single channel ammonia permeability, p_{NH_3} for nod26 of 12.7 (±0.6) $\times 10^{-15}$ cm^3/subunit/s ($n = 3$) was calculated. Based on previous measurements, the single channel water permeability, p_f, for nod26 is 3.8×10^{-15} cm^3/subunit/s, suggesting a fourfold preference for the transport of ammonia. This is supported by the P_{NH_3}/P_f ratio (4.9-fold) measured in the present study (Table 1).

4. Discussion

Given the similarities in van der Waals volume for water (12.4 cm^3/mol) and NH_3 (13.8 cm^3/mol) and similarities in their

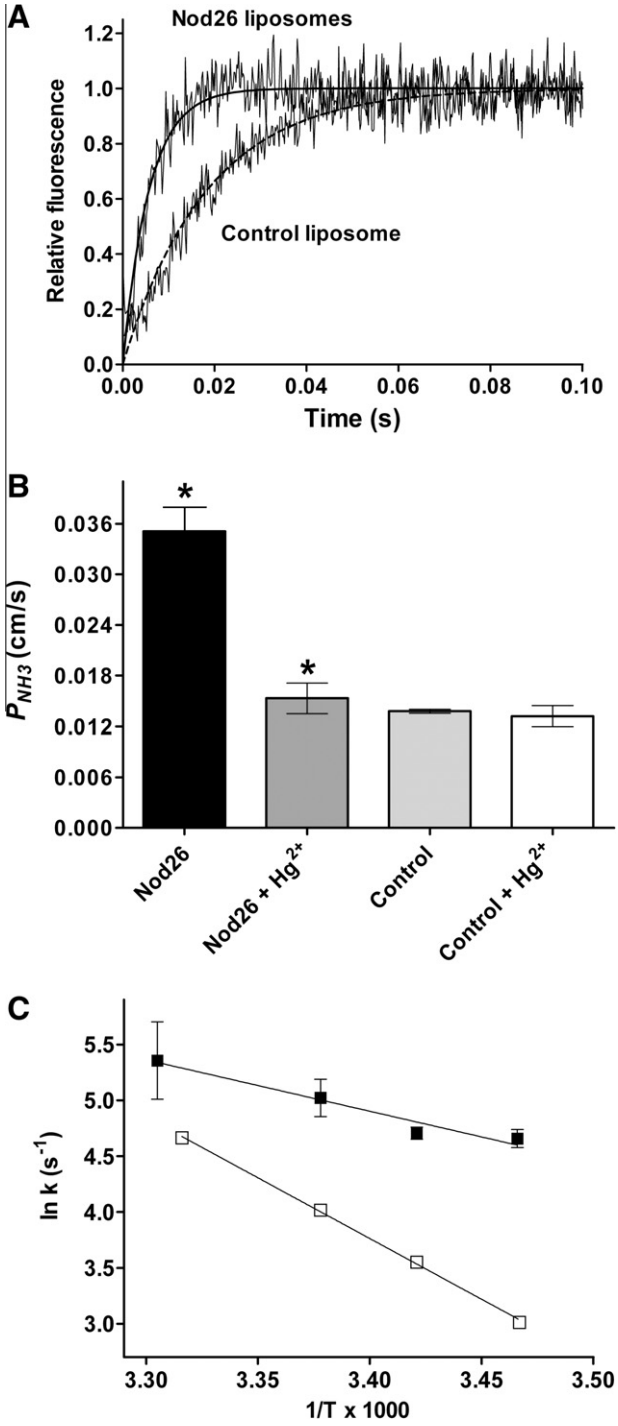

Fig. 2. Ammonia (NH_3) permeability measurements of nod26-proteoliposomes. (A) Time-course of fluorescence increase in CF-loaded nod26 proteoliposomes and negative control liposomes upon injection into 5 mM NH_4Cl was measured by stopped-flow fluorimetry at 23 °C. The data represent an average of five injections and the curve fit to a single exponential is shown. (B) Ammonia (NH_3) permeabilities (P_{NH_3}) of nod26 proteoliposomes and control liposomes were calculated from stopped flow measurements in the presence or absence of 1 mM $HgCl_2$. The error bars show the standard error of the mean ($n = 13$) for nod26, ($n = 8$) for nod26 with $HgCl_2$, ($n = 9$) for negative control, and ($n = 4$) for negative control with $HgCl_2$. (* indicates P value <0.0001). (C) Arrhenius plots of NH_3 uptake from nod26 proteoliposomes (■) and negative control liposomes (□) are shown. The natural log of the rate constants (ln k) were determined from the single exponential curve fits of fluorescence traces. Error bars show standard error of the mean of three to six replicates.

dipole moments (1.471 D for NH_3 and 1.854 D for H_2O), it could be argued that NH_3 transport is a property shared by all aquaporins.

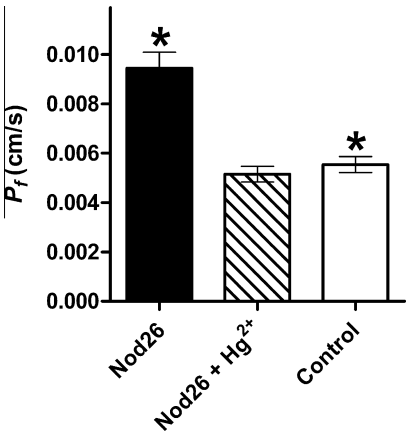

Fig. 3. Osmotic water permeability measurements of nod26-proteoliposomes. The osmotic water permeabilities (P_f) of nod26 proteoliposomes in the presence or absence of 1 mM $HgCl_2$ and negative control liposomes were determined as described in Section 2. Error bars show standard error of the mean ($n = 19$) for nod26, ($n = 6$) for nod26 with $HgCl_2$, and ($n = 7$) for control. * indicates P value <0.002.

However, comparison of the transport selectivities of various aquaporins shows that this is not the case, and that the ability to select for water or ammonia transport is a property of the amino acids present within the aromatic/arginine (ar/R) selectivity filter [19–21]. This region is composed of a confluence of four amino acids that form the narrowest constriction within the pore and determine the selectivity of MIP/aquaporin transporters. Dynowski and Ludewig [20] investigated the molecular determinants of ammonia transport through plant aquaporins by using molecular dynamics simulations and by yeast complementation analyses on ammonia selective media. The water-selective AtPIP2;1, which transports water but not NH_3, was used as a scaffold for site-directed mutagenesis to construct ar/R regions characteristic of various Arabidopsis NIP transporters. The results show that several NIP-like mutants of both the NIP I and NIP II ar/R subclasses show the ability to complement yeast ammonia auxotrophs but that this ability also depends upon additional residues in other regions of the pore [20].

In the present study it is shown that purified soybean nod26, the NIP family archetype which has an ar/R region characteristic of NIP I pores [22], exhibits the ability to transport NH_3 and shows an approximately fourfold stronger preference for this substrate over water. Additionally, the use of purified nod26 liposomes allowed a determination of the single channel rate for ammonia transport. The calculated p_{NH_3} of nod26 (1.27×10^{-14} cm^3/s) is comparable to the value obtained by other ammonia transporting aquaporins such as AQP8 ($p_{NH_3} = 2.7 \times 10^{-14}$ cm^3/sec) [23]. Assuming one transport channel per nod26 monomer, this represents a permeability of 3×10^8 NH_3 molecules per channel per sec. Overall, the findings in the present report support previous work with NIP-like ar/R mutants [20] and suggest that ammonia transport is among the multifunctional transport activities associated with NIP proteins.

Soybean nod26 is a SM-specific protein constituting a large percentage of the protein complement of this specialized membrane [6–8]. Based on the density of nod26 on the SM [8], and the calculated p_{NH_3}, the presence of nod26 on the SM is more than adequate to account for the channel mediated flux of NH_3 across the soybean SM previously reported by Niemietz and Tyerman [11]. Further, similar to facilitated NH_3 transport in SM vesicles, the nod26 NH_3 permeability shows a reduction in activation energy as well as mercurial sensitivity in contrast to diffusion through lipid bilayers.

Based on previous reports [8–9,11] and the present findings, soybean nod26 appears to be the principal protein on the symbiosome responsible for water and NH_3 permeabilities. Less certain however,

are the metabolic and/or osmoregulatory roles of these activities in the symbiosis, and how these two activities are regulated in response to environmental and metabolic cues. With respect to ammonia permeability, it is attractive to propose a role for nod26 as a potential efflux pathway for fixed NH_3 from the symbiosome. The efflux of fixed nitrogen from the symbiosome space to the infected cell cytosol is mediated by SM transport by one of the two potential mechanisms: 1. Directional transport of NH_4^+ cations to the cytosol by an inwardly rectified, voltage-activated non-selective cation channel [24]; or 2. Efflux of uncharged NH_3 through the SM with nod26 providing a low energy pathway for this movement. The relative contributions of these pathways depends upon the pH of the symbiosome space and cytosolic compartments, the concentration gradient of NH_4^+ between the symbiosome and cytosolic compartments, and the resting potential of the SM, which is primarily controlled by an energizing H^+-pumping ATPase (discussed in [11]). Under conditions of high H^+-ATPase activity, the hyperpolarization of the SM and acidification of the symbiosome space would predominantly favor the efflux of fixed nitrogen in the form of NH_4^+ through voltage-activated non-selective cation channels [24]. Movement of NH_3 across the SM to the cytosolic compartment would be favored under conditions of low H^+-ATPase activity which would result in a less energized SM and less acidic conditions in the symbiosome space. Additional support for a nod26 role in fixed nitrogen transport comes from the observation that it forms a complex with soybean glutamine synthetase, the principal enzyme involved in nitrogen assimilation [25]. This raises the possibility that efflux of NH_3 through the nod26 channel would be rapidly assimilated on the cytosolic side of the SM by bound glutamine synthetase, helping to reduce cytosolic NH_3 levels and the possibility of ammonia toxicity.

With respect to regulation, comparison of the P_{NH_3}/P_f between isolated SM and recombinant nod26 in proteoliposomes suggests possible modulation of water and ammonia transport activities of the protein on the SM. For example, the P_{NH_3}/P_f (0.8–1.4) reported for isolated SM vesicles [11] is lower than the fivefold NH_3 preference calculated in the present study with isolated recombinant nod26. One factor that could explain this difference in permeability is posttranslational phosphorylation of native SM nod26. Soybean nod26 is phosphorylated on C-terminal Ser262 by an SM associated calcium-dependent protein kinase (CDPK) [7]. Previous observations show that CDPK phosphorylation of nod26 is regulated in response to developmental cues, with phosphorylation of the protein becoming apparent upon maturation of the infected cell and the ability to fix nitrogen [10]. In addition, nod26 becomes hyperphosphorylated in response to osmotic stresses such as soil salinity and drought [10], stimuli which coordinately regulate nitrogen fixation rates in nodules as well. Phosphorylation of nod26 results in an approximately threefold stimulation of the P_f of the protein [10]. The effects of phosphorylation on the NH_3 transport activity of nod26 remain unknown. However, preincubation of SM with ATP, a treatment that is known to trigger phosphorylation of the protein in situ [7], was found to stimulate the P_f of SM vesicles while conversely inhibiting the P_{NH_3} [11], suggesting a possible opposing effect of phosphorylation on water and ammonia transport activities. Whether phosphorylation modulates the selectivity of nod26 in response to metabolic (NH_3 transport) and osmoregulatory (water transport) cues merits further consideration.

Acknowledgment

Supported by National Science Foundation Grant MCB-0618075 to DMR.

References

[1] Roth, E., Jeon, K. and Stacey, G. (1988) Homology in endosymbiotic systems: the term 'symbiosome' in: Molecular Genetics of Plant Microbe (Palcios, R. and Verma, D.P.S., Eds.), pp. 220–225, ADS Press, St. Paul.
[2] Udvardi, M.K. and Day, D.A. (1997) Metabolite transport across symbiotic membranes of legume nodules. Annu. Rev. Plant Physiol. Plant Mol. Biol. 48, 493–523.
[3] Day, D.A., Poole, P.S., Tyerman, S.D. and Rosendahl, L. (2001) Ammonia and amino acid transport across symbiotic membranes in nitrogen-fixing legume nodules. Cell Mol. Life Sci. 58, 61–71.
[4] Fortin, M.G., Zelechowska, M. and Verma, D.P. (1985) Specific targeting of membrane nodulins to the bacteroid-enclosing compartment in soybean nodules. EMBO J. 4, 3041–3046.
[5] Catalano, C.M., Lane, W.S. and Sherrier, D.J. (2004) Biochemical characterization of symbiosome membrane proteins from *Medicago truncatula* root nodules. Electrophoresis 25, 519–531.
[6] Fortin, M.G., Morrison, N.A. and Verma, D.P. (1987) Nodulin-26, a peribacteroid membrane nodulin is expressed independently of the development of the peribacteroid compartment. Nucleic Acids Res. 15, 813–824.
[7] Weaver, C.D., Crombie, B., Stacey, G. and Roberts, D.M. (1991) Calcium-dependent phosphorylation of symbiosome membrane proteins from nitrogen-fixing soybean nodules: evidence for phosphorylation of nodulin-26. Plant Physiol. 95, 222–227.
[8] Rivers, R.L., Dean, R.M., Chandy, G., Hall, J.E., Roberts, D.M. and Zeidel, M.L. (1997) Functional analysis of nodulin 26, an aquaporin in soybean root nodule symbiosomes. J. Biol. Chem. 272, 16256–16261.
[9] Dean, R.M., Rivers, R.L., Zeidel, M.L. and Roberts, D.M. (1999) Purification and functional reconstitution of soybean nodulin 26. An aquaporin with water and glycerol transport properties. Biochemistry 38, 347–353.
[10] Guenther, J.F., Chanmanivone, N., Galetovic, M.P., Wallace, I.S., Cobb, J.A. and Roberts, D.M. (2003) Phosphorylation of soybean nodulin 26 on serine 262 enhances water permeability and is regulated developmentally and by osmotic signals. Plant Cell 15, 981–991.
[11] Niemietz, C.M. and Tyerman, S.D. (2000) Channel-mediated permeation of ammonia gas through the peribacteroid membrane of soybean nodules. FEBS Lett. 465, 110–114.
[12] Jahn, T.P., Møller, A.L., Zeuthen, T., Holm, L.M., Klaerke, D.A., Mohsin, B., Kuhlbrandt, W. and Schjoerring, J.K. (2004) Aquaporin homologues in plants and mammals transport ammonia. FEBS Lett. 574, 31–36.
[13] Litman, T., Sogaard, R. and Zeuthen, T. (2009) Ammonia and urea permeability of mammalian aquaporins. Handbook Exp. Pharmacol. 327, 58.
[14] Ludewig, U. and Dynowski, M. (2009) Plant aquaporin selectivity: where transport assays, computer simulations and physiology meet. Cell. Mol. Life Sci. 66, 3161–3175.
[15] Wu, S. and Letchworth, G.J. (2004) High efficiency transformation by electroporation of *Pichia pastoris* pretreated with lithium acetate and dithiothreitol. Biotechniques 36, 152–154.
[16] Karlsson, M., Fotiadis, D., Sjövall, S., Johansson, I., Hedfalk, K., Engel, A. and Kjellbom, P. (2003) Reconstitution of water channel function of an aquaporin overexpressed and purified from *Pichia pastoris*. FEBS Lett. 537, 68–72.
[17] Boron, W.F. and De Weer, P. (1976) Intracellular pH transients in squid giant axons caused by CO_2, NH_3, and metabolic inhibitors. J. Gen. Physiol. 67, 91–112.
[18] Vincill, E.D., Szczyglowski, K. and Roberts, D.M. (2005) GmN70 and LjN70. Anion transporters of the symbiosome membrane of nodules with a transport preference for nitrate. Plant Physiol. 137, 1435–1444.
[19] Beitz, E., Wu, B., Holm, L.M., Schultz, J.E. and Zeuthen, T. (2006) Point mutations in the aromatic/arginine region in aquaporin 1 allow passage of urea, glycerol, ammonia, and protons. Proc. Natl. Acad. Sci. USA 103, 269–274.
[20] Dynowski, M., Mayer, M., Moran, O. and Ludewig, U. (2008) Molecular determinants of ammonia and urea conductance in plant aquaporin homologs. FEBS Lett. 582, 2458–2462.
[21] Holm, L.M., Jahn, T.P., Møller, A.L., Schjoerring, J.K., Ferri, D., Klaerke, D.A. and Zeuthen, T. (2005) NH_3 and NH_4^+ permeability in aquaporin-expressing Xenopus oocytes. Pflugers Arch. 450, 415–428.
[22] Wallace, I.S. and Roberts, D.M. (2004) Homology modeling of representative subfamilies of Arabidopsis major intrinsic proteins. Classification based on the aromatic/arginine selectivity filter. Plant Physiol. 135, 1059–1068.
[23] Saparov, S.M., Liu, K., Agre, P. and Pohl, P. (2007) Fast and selective ammonia transport by aquaporin-8. J. Biol. Chem. 282, 5296–5301.
[24] Tyerman, S.D., Whitehead, L.F. and Day, D.A. (1995) A channel-like transporter for NH_4^+ on the symbiotic interface of N_2-fixing plants. Nature 378, 629–632.
[25] Masalkar, P., Wallace, I.S., Hwang, J.H. and Roberts, D.M. (2010) Interaction of cytosolic glutamine synthetase of soybean root nodules with the C-terminal domain of the symbiosome membrane nodulin 26 aquaglyceroporin. J. Biol. Chem. 285, 23880–23888.